Focussing of an electron ring in the presence of a squirrel cage and conducting cylinder

I. Hofmann

IPP 0/16 March 1973

MAX-PLANCK-INSTITUT FÜR PLASMAPHYSIK

GARCHING BEI MÜNCHEN

MAX-PLANCK-INSTITUT FÜR PLASMAPHYSIK

GARCHING BEI MÜNCHEN

Focussing of an electron ring in the presence of a squirrel cage and conducting cylinder

I. Hofmann

IPP 0/16 March 1973

Die nachstehende Arbeit wurde im Rahmen des Vertrages zwischen dem Max-Planck-Institut für Plasmaphysik und der Europäischen Atomgemeinschaft über die Zusammenarbeit auf dem Gebiete der Plasmaphysik durchgeführt.

IPP 0/16 I. Hofmann Focussing of an electron ring in the presence of a squirrel cage and conducting cylinder.

Abstract

The focussing fields due to image charges and - currents on a squirrel-cage-type conductor outside a relativistic electron ring and on a conducting cylinder inside the ring are calculated, using a thin ring approximation. The resulting image contributions are then compared with the self-field effects and an estimate is given for the Landau-damping coefficient.

I. Introduction

In the acceleration or pre-acceleration phase focussing of the axial betatron oscillations in a relativistic electron ring may no longer be ensured by the external guide field because its contribution may be weak compared with the repulsive self-field effects.

The stabilizing effect exerted on axial betatron oscillations by images on metallic conductors or dielectrics close to the ring has been investigated by several authors [3], [4], [5], [6]. In [2] the stabilization due to a squirrel-cage-type conductor was first proved to be useful.

In the present paper the focussing properties of a system composed of both a squirrel cage and a conducting cylinder are investigated. We study their influence on radial and axial betatron oscillations within the framework of a test-particle model and compare the results with the effects due to the self-fields of the electron ring, applying the usual approximation for the toroidal effects [4]. The presence of an additional conducting cylinder inside the electron ring may be required to produce a B_φ -field or be desirable for stabilizing negative-mass instabilities, which calls for good azimuthal conductivity.

II. Model

To calculate image quantities (part III) we represent the ER as a thin circular current ring A concentric with a squirrel cage B and a conducting cylinder C. B consists of N cylindrically ordered metallic ribbons and contains C, whereas A lies between both and is assumed to be at rest in our system of reference.

The thin-ring model will be relaxed in part IV when the self-fields of the ring are calculated.

It should be noted that for calculating images the assumption of a thin ring ($\varrho \ll a$) is evidently justified as long as $\varrho \ll$ min (a-c, b-a). If it is borne in mind that in plane geometry (i.e. a, b, c $\to \infty$, but a-c, b-a fixed) the small ring radius has no influence upon the image fields, and that the contribution of the squirrel cage to the image fields (which is greater than that of the cylindrical conductor) is only weakly dependent on curvature, being mainly dependent on the anisotropy of the conductivity, reasonably good results may be expected with our model also if $\varrho \lesssim$ min (a-c, b-a).

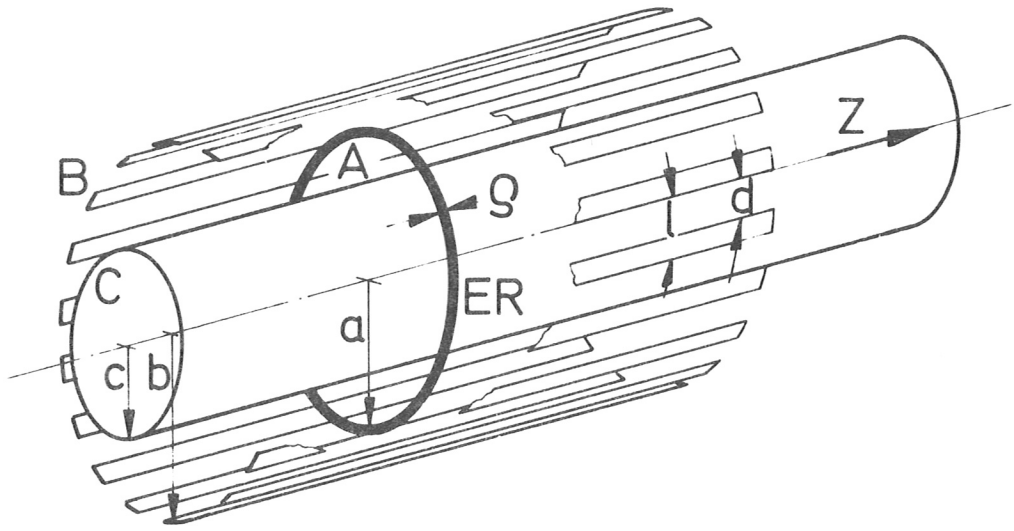

a: ring radius

b: squirrel-cage radius

c: cylinder radius

N: number of ribbons

d: width of slits

l-d: width of ribbons

$l = \frac{2c\pi}{N}$

Θ: $\frac{l-d}{l}\pi$ angle corresponding to metallic ribbon $(0 < \Theta < \pi)$

I: ring current [e.s.u]

Q: total ring charge [e.s.u] $(= en \cdot 2a\pi)$

III. Derivation of the fields due to images

With the model specified above we calculate fields and field gradients at the centre of the electron ring, following a method which was prescribed by [1], [2] in the case where only a squirrel cage was present.

1. Expressions for the potentials

In cylindrical geometry we obtain from the Maxwell equations the following well-known expressions for the electrostatic potentials and the vector potential in terms of Modified Bessel Functions I_n, K_n [7] (we assume electrostatic units and c = 1):

a) Sources

With a charge density $\varrho(r,\varphi,z) = \delta(z)\,\delta(a-r)\,e\,n$ and a current $j_\varphi(r,\varphi,z) = \delta(z)\,\delta(a-r)\,I$, where $I = e\,n\,v_\varphi$ (v_φ azimuthal velocity of electrons in units of c), we get from $\phi = \int \frac{\varrho(x')}{|x-x'|}\,d^3x'$ and $\underset{\rightarrow}{A} = \int \frac{\underset{\rightarrow}{j}(x')}{|x-x'|}\,d^3x'$ the source contributions (ring self-fields):

$$(1)\quad \phi^{(A)} = 2e\,n\,a \int_{-\infty}^{\infty} dk\, e^{ikz} \begin{cases} J_0(|k|r)\,K_0(|k|a) & r \le a \\ K_0(|k|r)\,J_0(|k|a) & r \ge a \end{cases}$$

$$\underset{\rightarrow}{E} = -\nabla\phi^{(A)}$$

$$(2)\quad A_\varphi^{(A)} = 2a\,I \int_{-\infty}^{\infty} dk\, e^{ikz} \begin{cases} J_1(|k|r)\,K_1(|k|r) & r \le a \\ K_1(|k|r)\,J_1(|k|a) & r \ge a \end{cases}$$

$$A_r^{(A)} = A_z^{(A)} \equiv 0\,,$$

$$\underset{\rightarrow}{B}^{(A)} = \nabla \times \underset{\rightarrow}{A}^{(A)}$$

b) Images

The potentials due to the images on the walls can be written:

$$(3)\quad \phi^{(B)} = -2e\,n\,b \sum_{m=-\infty}^{\infty} \int_{-\infty}^{\infty} dk\, e^{ikz+imN\varphi}\, a_m(b) \cdot \begin{cases} J_{Nm}(|k|r)\,K_{Nm}(|k|b) & r \le b \\ K_{Nm}(|k|r)\,J_{Nm}(|k|b) & r \ge b \end{cases}$$

$$(4)\quad A_r^{(B)} = I \sum_{m=-\infty}^{\infty} \int_{-\infty}^{\infty} dk\, e^{ikz+imN\varphi} \begin{cases} C_m(k)\,J_{mN}(|k|r) & r \le b \\ D_m(k)\,K_{mN}(|k|r) & r \ge b \end{cases}$$

$$(5)\quad A_\varphi^{(B)} = -I \sum_{m=-\infty}^{\infty} \int_{-\infty}^{+\infty} dk\,|k|\, e^{ikz+imN\varphi} \begin{cases} C_m(k)\,J'_{mN}(|k|r) & r \le b \\ D_m(k)\,K'_{mN}(|k|r) & r \ge b \end{cases}$$

$$A_z^{(B)} \equiv 0$$

for the images on the squirrel cage (B), and

$$(6)\quad \phi^{(C)} = -2e\,n\,b \sum \int dk\, e^{ikz+imN\varphi}\, \bar{a}_m(k) \begin{cases} J_{Nm}(|k|r)\,K_{Nm}(|k|c) & r \le c \\ K_{Nm}(|k|r)\,J_{Nm}(|k|b) & r \ge c \end{cases}$$

$$(7)\quad A_r^{(C)} = I \sum_{m=-\infty}^{\infty} \int_{-\infty}^{\infty} dk\, e^{ikz+im N\varphi} \cdot \begin{cases} \bar{C}_m(k)\, J_{mN}(|k|r) & r \le c \\ \bar{D}_m(k)\, K_{mN}(|k|r) & r \ge c \end{cases}$$

$$(8)\quad A_\varphi^{(C)} = -I \sum_{m=-\infty}^{+\infty} \int_{-\infty}^{+\infty} dk\, |k|\, e^{ikz+im N\varphi} \cdot \begin{cases} \bar{C}_m(k)\, J'_{mN}(|k|r) & r \le c \\ \bar{D}_m(k)\, K'_{mN}(|k|r) & r \ge c \end{cases}$$

$$A_z^{(C)} = 0$$

for the images on the cylinder (C).

In these expressions we have used the fact that because of symmetry only harmonics of the order m . N($m = 0, \pm 1, \pm 2, \ldots$) give a non vanishing contribution; this allows us to substitute $N\varphi \to \varphi$, with $-\pi < \varphi < \pi$. Then $|\varphi| \le \theta$ corresponds to points on the metallic ribbon and $\theta < |\varphi| < \pi$ corresponds to points on the slit.

The total potentials are

$$\phi = \phi^{(A)} + \phi^{(B)} + \phi^{(C)}, \qquad \underset{\rightarrow}{A} = \underset{\rightarrow}{A}^{(A)} + \underset{\rightarrow}{A}^{(B)} + \underset{\rightarrow}{A}^{(C)}$$

2. Solution of the boundary value problem

We require that $E_\parallel = 0$, $B_\perp = 0$ on the metallic (perfectly conducting) surfaces and that E, B be continuous across the slits of the squirrel cage. Thus we obtain for the potentials:

a) Continuity conditions

For $r = b$, $\theta < |\varphi| < \pi$ we have $\left[\frac{\partial \phi}{\partial r}\right]_{b-0}^{b+0} = 0$, and so by inserting (1), (3), (6) and using $J_n(v)\, K'_n(v) - J'_n(v)\, K_n(v) = \frac{1}{v}$ (see 8) we get:

$$(9)\quad \sum_{m=-\infty}^{\infty} a_m(k)\, e^{im\varphi} = 0$$

From $\left[\frac{\partial A_\varphi}{\partial z}\right]_{b-0}^{b+0} = 0$ we obtain

$$(10)\quad \begin{aligned} D_m(k) &= c_m(k)\, J'_{mN}(|k|b) \\ C_m(k) &= c_m(k)\, K'_{mN}(|k|b) \end{aligned}$$

and from $\left[A_\varphi + r\frac{\partial A_\varphi}{\partial r} - \frac{\partial A_r}{\partial \varphi}\right]_{b-0}^{b+0} = 0$ with (10):

(11) $$\sum_{m=-\infty}^{\infty} C_m(k)\, e^{im\varphi} = 0$$

b) Conditions on conductors

α) $r = c$ (cylinder)

From $\phi = 0$, $|\varphi| \le \pi$ we get

$$\sum e^{im\varphi}\left(\beta\, a_m(k) K_{mN}(|k|\beta) + c\cdot \bar{a}_m(k) K_{mN}(|k|c)\right) J_{mN}(|k|c) = a\, J_0(|k|c) K_0(|k|c)$$

(12) and thus $$\bar{a}_0(k) = \frac{a K_0(|k|a) - \beta\, a_0(k) K_0(|k|\beta)}{c\cdot K_0(|k|\beta)}$$

(13) $$\bar{a}_m(k) = -\frac{\beta}{c}\,\frac{K_{mN}(|k|\beta)}{K_{mN}(|k|c)}\, a_m(k) \qquad (m \neq 0)$$

From $\frac{\partial A_\varphi}{\partial z} = 0$, $|\varphi| \le \pi$ it follows that

(14) $$\bar{C}_m(k) = -C_m(k)\,\frac{K'_{mN}(|k|\beta)}{K'_{mN}(|k|c)} \qquad (m \neq 0)$$

(15) $$\bar{C}_0(k) = -\frac{2a}{|k|}\,\frac{K_1(|k|a)}{K_1(|k|c)} - C_0(k)\,\frac{K_1(|k|\beta)}{K_1(|k|c)}$$

with $$\bar{C}_m(k) = \bar{c}_m(k)\, J'_{mN}(|k|c)$$

β) $r = b$ (squirrel cage)

$\phi = 0$ for $|\varphi| \le \Theta$, thus

(16) $$\sum_{m=-\infty}^{+\infty}\left(\beta\cdot a_m(k) J_{mN}(|k|\beta) + c\,\bar{a}_m(k) J_{mN}(|k|c)\right) K_{mN}(|k|\beta)\, e^{im\varphi} = a\, I_0(|k|\beta) K_0(|k|a)$$

$\frac{\partial A_\varphi}{\partial z} = 0$ for $|\varphi| \le \Theta$, thus

(17) $$\sum\left(C_m(k) J'_{mN}(|k|\beta) + \bar{C}_m(k) J'_{mN}(|k|c)\right) K'_{mN}(|k|\beta)\, e^{im\varphi} = \frac{2aI}{|k|} J_1(|k|a) K_1(|k|\beta)$$

By eliminating $\bar{a}_m(k)$ and $\bar{c}_m(k)$ we thus find the following two infinite systems of equations for the unknown coefficients $a_m(k)$, $c_m(k)$:

$$(18a)\quad \sum_{m=-\infty}^{\infty} a_m(k)\, e^{im\varphi} = 0 \qquad (\theta < |\varphi| < \pi)$$

$$(18b)\quad \sum_{-\infty}^{\infty} a_m(k)\, J_{mN}(k|b)\, K_{mN}(k|\theta)\left(1 - \frac{K_{mN}(k|\theta)}{K_{mN}(k|a)}\,\frac{J_{mN}(k|c)}{J_{mN}(k|\theta)}\right) e^{im\varphi} =$$

$$= \frac{a}{6}\, K_0(k|\theta)\, J_0(k|a)\left(1 - \frac{K_0(k|a)\, J_0(k|c)}{K_0(k|c)\, J_0(k|a)}\right) \qquad (|\varphi| \le \theta)$$

$$(19a)\quad \sum_{-\infty}^{\infty} c_m(k)\, e^{im\varphi} = 0 \qquad (\theta < |\varphi| < \pi)$$

$$(19b)\quad \sum c_m(k)\, J'_{mN}(k|\theta)\, K'_{mN}(k|\theta)\left(1 - \frac{K'_{mN}(k|\theta)}{K'_{mN}(k|c)}\,\frac{J'_{mN}(k|c)}{J'_{mN}(k|\theta)}\right) e^{im\varphi} =$$

$$(|\varphi| \le \theta) \qquad = \frac{2a}{|k|}\, J_1(k|a)\, K_1(k|\theta)\left(1 - \frac{K_1(k|a)\, J_1(k|c)}{K_1(k|c)\, J_1(k|a)}\right)$$

Since the infinite series in (18) - (19) do not converge uniformly in , approximate solutions cannot be obtained for the lowest order Fourier coefficients $c_0(k)$, $a_0(k)$ simply by truncating the infinite series at some finite order. This is a well-known problem in the theory of diffraction of waves from plane gratings.
Next we write either set of equations (19), (20) in standard form:

$$(20)\quad \sum_{n\neq 0} x_n(k)\, e^{in\varphi} = 0 \qquad \text{(by differentiation of (18a) or (19a))}$$

$$(21)\quad \sum_{n\neq 0} x_n(k)\, \frac{n}{|n|}\,(1 - \varepsilon_n(k))\, e^{in\varphi} = \alpha(k) - x_0(k)\,\beta(k)$$

with the unknowns $x_n(k)$ and coefficients $\varepsilon_n(k)$, $\alpha(k)$, $\beta(k)$ being defined as follows:
Electric field: $x_0(k) \equiv a_0(k)$,

$$x_n(k) \equiv 2N\, J_0(k|b)\, K_0(k|\theta)\left(1 - \frac{K_0(k|\theta)\, J_0(k|c)}{K_0(k|c)\, J_0(k|\theta)}\right) a_0(k) - 2N\,\frac{a}{6}\, K_0(k|\theta)\, J_0(k|a)\left(1 - \frac{K_0(k|a)\, J_0(k|c)}{K_0(k|c)\, J_0(k|a)}\right) \qquad (n \neq 0)$$

$$\alpha(k) \equiv -\frac{a}{6}\,\frac{J_0(k|a)\, K_0(k|c) - K_0(k|a)\, J_0(k|c)}{J_0(k|\theta)\, K_0(k|c) - K_0(k|\theta)\, J_0(k|c)}, \qquad \beta(k) = \frac{1}{2N}\,\frac{K_0(k|c)/K_0(k|b)}{K_0(k|c)\, J_0(k|\theta) - K_0(k|\theta)\, J_0(k|c)}$$

$$\varepsilon_m(k) \equiv 1 - \frac{K_{mN}(|k|c)/K_{mN}(|k|b)}{2N|m|\left(J_{mN}(|k|b)K_{mN}(|k|c) - K_{mN}(|k|b)J_{mN}(|k|c)\right)}$$

Magnetic field

$$x_0(k) \equiv c_0(k) \quad , \quad x_n(k) \equiv n \cdot c_n(k) \quad (n \neq 0)$$

$$\alpha(k) \equiv -\frac{4a\beta^2|k|}{Nc} J_1(|k|a)K_1(|k|b)\left(1 - \frac{K_1(|k|a)J_1(|k|c)}{K_1(|k|c)J_1(|k|a)}\right)$$

$$\beta(k) \equiv \frac{2k^2\beta^2}{N} J_1(|k|b)K_1(|k|b)\left(1 - \frac{K_1(|k|b)J_1(|k|c)}{K_1(|k|c)J_1(|k|b)}\right)$$

$$\varepsilon_m(k) \equiv 1 + \frac{2k^2\beta^2}{N|m|} K'_{mN}(|k|b)J'_{mN}(|k|b)\left(1 - \frac{K'_{mN}(|k|b)J'_{mN}(|k|c)}{K'_{mN}(|k|c)J'_{mN}(|k|b)}\right)$$

The $\varepsilon_n(k)$ have the important property $\varepsilon_n(k) \to 0$, $(k \to 0)$, as follows from the asymptotic behaviour of modified Bessel functions:

$$J_n(x) \sim \frac{1}{\Gamma(n+1)}\left(\frac{x}{2}\right)^n \quad , \quad K_n(x) \sim \frac{1}{2}\Gamma(n)\left(\frac{2}{x}\right)^n \quad (x \to 0,\ n \neq 0)$$

Hence we may write equation (21) in the following form:

$$(21') \quad \sum_{n\neq 0} x_n(k) \frac{\kappa}{|n|} e^{in\varphi} = f(e^{i\varphi}) - x_0(k)\beta(k)$$

with

$$(22) \quad f(e^{i\varphi}) = \sum_{n\neq 0} x_n(k) \frac{n}{|n|} \varepsilon_n(k) e^{in\varphi} + \alpha(k)$$

Considering $f(e^{i\varphi})$ for the moment as a known expression, eqs. (20), (21') constitute the Riemann-Gilbert problem, which allows explicit solution of the $x_n(k)$ in terms of the $\beta(k)$ and Fourier coefficients of $f(e^{i\varphi})$ by integrating the expressions in eqs. (20), (21') along appropriate contours in the complex ζ -plane ($\zeta = re^{i\varphi}$) and Fourier analyzing. For details of this procedure see [1].

We thus obtain the following expressions for $x_n(k)$, which are, of course, not explicit in $x_n(k)$ because of eq.(22), except in the limit $k \to 0$, where $f \to \alpha(k)$:

$$(23)\qquad \begin{aligned} x_n(k) &= \sum_{m\neq 0} x_m \frac{m}{|m|} \varepsilon_m(k) V_n^m + \alpha(k) V_n^0 - x_0(k)\beta(k) V_n^0 + 2\gamma R_n \qquad (n\neq 0) \\ 0 &= \sum_{m\neq 0} x_m \frac{m}{|m|} \varepsilon_m(k) V_0^m + \alpha(k) V_0^0 - x_0(k)\beta(k) V_0^0 + 2\gamma R_0 \\ x_0(k) &= -\sum x_m \frac{m}{|m|} \varepsilon_m(k) V_\sigma^m - \alpha(k) V_\sigma^0 + x_0(k)\beta(k) V_\sigma^0 - 2\gamma R_\sigma \end{aligned}$$

with the following definitions: (1))

$$V_n^m = \frac{1}{2\pi} \int_{-\pi}^{+\pi} V_m(e^{i\varphi})\, R(e^{i\varphi})\, e^{-in\varphi}\, d\varphi$$

$$V_\sigma^m = \frac{i}{2\pi} \int_{-\pi}^{\pi} \varphi\, V_m(e^{i\varphi})\, R(e^{i\varphi})\, d\varphi$$

$$R_m = \frac{1}{2\pi} \int_{-\pi}^{\pi} R(e^{i\varphi})\, e^{-im\varphi}\, d\varphi$$

$$R_\sigma = \frac{i}{2\pi} \int_{-\pi}^{\pi} \varphi\, R(e^{i\varphi})\, d\varphi$$

$$V_n(\zeta_0) = \frac{1}{\pi i} \int_{\substack{|\zeta|=1 \\ -\Theta<\arg\zeta<\Theta}} \frac{\zeta^n}{\zeta-\zeta_0} \sqrt{(\zeta-e^{i\Theta})(\zeta-e^{-i\Theta})}\, d\zeta \qquad -\Theta<\arg\zeta_0<\Theta$$

$$R(\zeta) = \begin{cases} \dfrac{1}{\sqrt{(\zeta-e^{i\Theta})(\zeta-e^{-i\Theta})}} & -\Theta<\arg\zeta<\Theta \\ 0 & |\arg\zeta| \geq \Theta \end{cases}$$

With $\Theta \equiv \frac{\ell-d}{\ell}\pi$ these integrals apply for the B-field case. For the E-field case we obtain the corresponding expressions by substituting Θ by $\pi - \Theta$. We remark that V_n may be expressed in terms of a finite sum of Legendre functions $P_s(\cos\Theta)$ for numerical calculation (see 1)). γ is an integration constant which may be eliminated from (23).

It is now important that in any finite domain of k ($0 \leq |k| \leq k_{max}$) the $\varepsilon_m(k)$ uniformly approach zero for $m \longrightarrow \infty$.

Therefore, we may set $\varepsilon_m(k) \equiv 0$ for $m > M_o$ (with M_o sufficiently large) and obtain a finite set of inhomogeneous linear equations in x_n ($n = 0 \ldots x_{M_o}$), which are solved numerically.

3. Calculation of image field quantities

When the method mentioned above is applied, solutions are found for the $a_m(k)$, $c_m(k)$ up to any order of the smallness parameter $\varepsilon_m(k)$, provided that k be restricted to $|k| \leq k_{max} < \infty$. This restriction is allowed in the expressions for the potentials because the integrals over k converge exponentially for $|k| \to \infty$.

For linear betatron oscillations it is sufficient to consider only the non-oscillating field contributions, i.e. the zero-order angular harmonics connected with $a_0(k)$, $c_0(k)$.

The potential produced by the images on the composite system of a squirrel cage and a cylinder may then be obtained by evaluating the following integrals:

$$(24)\quad \phi^{(0)} = -4en\beta \int_0^{k_{max}} dka\, \cos(kz) \Big\{ a_0(k) \Big[K_0(kb) J_0(kr) - \frac{K_0(kb)}{K_0(kc)} J_0(kc) K_0(kr) \Big] + \frac{a}{\beta} \frac{K_0(ka)}{K_0(kc)} J_0(kc)\, K_0(kr) \Big\}$$

$$(25)\quad A_\varphi^{(0)} = 2I \int_0^{k_{max}} dka\, k\, \cos(kz) \Big\{ c_0(k) \Big[K_1(kb) J_1(kr) - \frac{K_1(kb)}{K_1(kc)} J_1(kc) K_1(kr) \Big] - \frac{2a}{k} \frac{K_1(ka)}{K_1(kc)} J_1(kc)\, K_1(kr) \Big\}$$

$$A_r^{(0)} = 0$$

The values of fields and field gradients at the position of the ring may then be expressed in the following form, making use of $\operatorname{div} E = 0$ and $\nabla \times B = 0$:

$$E_r = \frac{Q}{a^2} \frac{2}{\pi} V_E \qquad Q := 2ena\pi$$

$$\frac{\partial E_z}{\partial z} = -\frac{Q}{a^3} \frac{2}{\pi} T_E$$

$$\frac{\partial E_r}{\partial r} = \frac{Q}{a^3} \frac{2}{\pi} (T_E - V_E)$$

$$B_z = -\frac{4I}{a} V_M \qquad I = \beta \frac{Q}{2\pi a}$$

$$\frac{\partial B_r}{\partial z} = -\frac{4I}{a^2} T_M$$

$$\frac{\partial B_z}{\partial r} = \frac{\partial B_r}{\partial z}$$

where the coefficients T, V depend on a, b, c only via $p \equiv \frac{a}{b}$, $q \equiv \frac{c}{b}$:

$$T_E = \rho^2 \int_0^{t_{max}} dt\, t^2 \left\{ a_0(t) \left[K_0(t) J_0(\rho t) - \frac{K_0(t)}{K_0(tq)} J_0(tq) K_0(tp) \right] + \rho \frac{K_0(tp)}{K_0(tq)} J_0(tq) K_0(tp) \right\}$$

$$T_M = -\frac{\rho^2}{2} \int_0^{t_{max}} dt\, t^3 \left\{ c_0(t) \left[K_1(t) J_1(tp) - \frac{K_1(t)}{K_1(tq)} J_1(tq) K_1(tp) \right] - \frac{2\rho}{t} \frac{K_1(tp)}{K_1(tq)} J_1(tq) K_1(tp) \right\}$$

$$V_E = \rho \int_0^{t_{max}} dt \left\{ a_0(t) \left[J_1(\rho t) K_0(t) + \frac{K_0(t)}{K_0(tq)} J_0(tq) K_1(tp) \right] - \rho \frac{K_0(tp)}{K_0(tq)} J_0(tq) K_1(tp) \right\}$$

$$V_M = -\frac{\rho}{2} \int_0^{t_{max}} dt \left\{ c_0(t) \left[J_0(\rho t) K_0(t) + \frac{K_1(t)}{K_1(tq)} J_1(tq) K_0(tp) \right] + \frac{2\rho}{t} \frac{K_1(tp)}{K_1(tq)} J_1(tq) K_0(tp) \right\}$$

with $t = b \cdot k$, $t_{max} = b \cdot k_{max}$

It should be noted that the notation of [3] is obtained if the following substitutions are made:

$p^{-1} \rightarrow S$, $V_E \rightarrow K$, $T_E \rightarrow Y$, $b \rightarrow T$, $a \rightarrow R$

$V_M \rightarrow L$, $T_M \rightarrow Z$

The above results agree with those derived by [2], where the additional cylinder was absent, if terms containing c are simply cancelled.

A change of the positions of the squirrel cage and cylinder (i.e. $p > 1$, $q < 1$) may be obtained merely by replacing $I_0 \rightarrow K_0$, $K_0 \rightarrow I_0$, $I_1 \rightarrow -K_1$, $K_1 \rightarrow -I_1$.

IV. Numerical evaluation and comparison of self-field and image-field effects

1. Numerical solution of the boundary value problems for electric and magnetic fields

In order to obtain the field coefficients $(a_o(t), c_o(t))$, the following Fortran computer program was written:

a) After introducing dimensionless parameters $p = \frac{a}{b}$, $q = \frac{c}{b}$, $t = kb$, we solve (23) for a given set of values for p, q, N, Θ, assuming $\varepsilon_m(t) \equiv 0$ for $m > M_o$ (thus yielding an inhomogeneous system of equations of order $M_o + 2$. A value of $M_o = 9$ gave sufficient accuracy within computer round-off. The (dimensionless) wavelength parameter t varies from t_{min} .... t_{max}, these limits being determined from convergence considerations of the Fourier integrals as will be discussed next.

b) The lowest-order Fourier coefficients resulting from (23), i.e. $a_o(t)$, $c_o(t)$, and the modified Bessel functions I_n, k_n are integrated according to eqs. (24) - (25). It is evident from the asymptotic behaviour of the modified Bessel functions $I_n(t)$, $K_n(t)$ for $t \to 0$ that all integrands are bounded for $t \to 0$, taking into account also the asymptotic behaviour of a_o, c_o, which results from eqs. (18), (19) as $a_o \sim 0(1)$, $c_o \sim 0(t^{-1})$ for $t \to 0$. Hence the indefiniteness of the integrand at t = 0 may be overcome simply by excluding a small neighbourhood of t = 0 (we chose $t_{min} = 0.1$).

The upper limit of integration t_{max} has to be chosen according to the following argumentation: from $I_n(\alpha t) \to (1/2\pi\alpha t)^{1/2} e^{\alpha t}$, $K_n(\beta t) \to (1/2\pi\beta t)^{1/2} e^{-\beta t}$ for $t \to \infty$ we get the asymptotic behaviour of the Fourier coefficients

$a_0(t) \sim e^{-t(1-p)}$, $c_0(t) \sim \frac{e^{-t(1-p)}}{t}$ using eqs. (18), (19).
Next it is seen that the integrands of any of the integrals (22) ... (25) converge more strongly than $\max\left(t^2 e^{2t(p-1)}, t^2 e^{2t(q-p)}\right)$ and so t_{max} is chosen according to $2t_{max} \cdot \min(p-1, q-p) = T$ with T (independent of p,q) sufficiently large (in our case $T = 10$). An integration step $dt = 0.1$ proved to yield sufficient accuracy.

2. Results

In fig. 1 - 3 we display the dependence of the axial focussing force constant $\frac{\partial F_z}{\partial z} \equiv \frac{\partial E_z}{\partial z} - \frac{\partial B_r}{\partial z}$ ($\beta = 1$) on the data of the squirrel cage in the case where no additional cylinder is present (except fig.3). We observe an optimal focussing effect for $\Theta = \pi/2$ and $N \gtrsim 30$ in agreement with [2].

In tables 1 - 3 the following quantities are listed for different sets of the parameters p, q, N, included the case where the squirrel cage is replaced by a cylinder:

$$a^3/Q \frac{\partial E_z}{\partial z}\ ,\ -\frac{a^2}{I}\frac{\partial B_r}{\partial z} = -\frac{a^2}{I}\frac{\partial B_z}{\partial r}\ ,\ \frac{a^2}{Q}E_r\ ,\ -\frac{a}{I}B_z\ ,\ \frac{a^3}{Q}\frac{\partial E_r}{\partial r}$$

and total forces ($\beta = 1$):

$$a^3/Q \frac{\partial F_z}{\partial z}\ ,\ \frac{a^2}{Q}F_r\ ,\ a^3/Q \frac{\partial F_r}{\partial r}$$

$$\epsilon_{1,E} \equiv \pi \frac{(b-a)^2 a}{2Q}\left(-\frac{\partial E_z}{\partial z}\right)\ ,\quad \epsilon_{1,M} \equiv \frac{(b-a)^2}{4I}\left(-\frac{\partial B_r}{\partial z}\right)$$

The $\epsilon_{1,E}$, $\epsilon_{1,M}$ are the electrostatic and magnetic image-field coefficients considered in [3].

3. Comparison with self-field effects and shift of betatron oscillation frequencies

With the results of 4) for ν_r, ν_z - including self-field effects - we obtain the following expressions:

$$(26)\quad \nu_r^2 = 1 - n - \mu\left\{\frac{2a^2}{\rho_1\bar{\rho}}\left(\frac{1}{\gamma^2}-f\right) - \frac{P}{2} + 4\frac{(1-f)\epsilon_{1,E} - \beta^2\epsilon_{1,M}}{(P^{-1}-1)^2} + n\left[\left(1-\tfrac{f}{2}\right)P + (1-f)K - \beta^2 L\right]\right\}$$

$$(27)\quad \nu_z^2 = n + \mu\left\{-\frac{2a^2}{\rho_2\bar{\rho}}\left(\frac{1}{\gamma^2}-f\right) - \frac{P}{2} + 4\frac{(1-f)\epsilon_{1,E} - \beta^2\epsilon_{1,M}}{(P^{-1}-1)^2} + n\left[\left(1-\tfrac{f}{2}\right)P + (1-f)K - \beta^2 L\right]\right\}$$

$$P = 2\ln\frac{\rho_a}{\bar{\rho}}$$

$$K = 2\pi\frac{a^2}{Q}E_y$$

$$L = -\frac{a}{I}B_z$$

n: field index

ρ_1, ρ_2 radii of elliptical cross section of the ring

$\bar{\rho} = (\rho_1 + \rho_2)/2$

f: $Z_{ion}\cdot\frac{N_{ion}}{N_{el}}$ fractional neutralisation

$\mu = \nu/\gamma$, $\nu = \frac{N_{el}\cdot r_0}{2\pi a}$, $r_0 = \frac{e^2}{m_0 c^2}$ classical electron radius

$\mu = 4.5\cdot 10^{-14}\cdot\frac{N_{el}}{a\gamma}$

We note that the terms on the right side of (26), (27) correspond to the following physical mechanisms: external field, straight-beam field, toroidal correction, image field, applied-field correction due to self-fields.

Assuming the following parameters for an ER :

$n = 0.02$

$a = 2.5$ cm

$\varrho_2 = 0.4$ cm

$\varrho_1 = 0.3$ cm

$\gamma = 25$

$N_{el} = 5 \cdot 10^{12}$

$f = 0$

$p = 0.8$

(no cylinder inside)

we obtain:

$$\nu_r^2 \approx 0.98 - \{0.0004 - 0.015 + 0.024 + 0.0007\} \approx 0.97$$

$$\nu_z^2 \approx 0.02 + \{-0.0005 - 0.015 + 0.024 + 0.0007\} \approx 0.03$$

4. Landau-damping coefficient

An approximate expression for the image contribution to the Landau-damping coefficient can be obtained as follows: From 4) the general expression for ν_r^2 is

$$\nu_r^2 = 1 - n + \frac{E_r + r\left(\frac{\partial E_r}{\partial r} + \beta \frac{\partial B_z}{\partial r}\right)}{B_{z_0} + E_{r_0}} = 1 - n + \nu_{r_{image}}^2$$

For small displacements $r = a + \delta r$ we obtain for the image contribution

$$\delta \nu_{r_{image}}^2 = \delta \left[r \frac{r\left(-\frac{\partial E_z}{\partial z} + \beta \frac{\partial B_z}{\partial r}\right)}{-en/\mu} \right]$$, where we used

div $E = 0$ and $B_{z_0} + E_{r_0} = -\frac{en}{\mu r_0}$

Thus $$\delta \nu_{r_{image}}^2 = \frac{2}{a} \delta r \, \nu_{r_{image}}^2 + \left. \frac{r^2 \frac{\partial}{\partial r}\left(-\frac{\partial E_z}{\partial z} + \beta \frac{\partial B_z}{\partial r}\right)}{-en/\mu} \right|_{r=a}$$

We calculate the derivatives with respect to r assuming a plane model with an image current at a distance of 2(b-a) from the source current and obtain

$$\frac{\partial}{\partial r}\left(\frac{\partial E_z}{\partial z}\right)_{r=a} = \frac{\partial}{\partial r}\left[\frac{\partial}{\partial z}\left(-\frac{2en \quad z}{(2(b-a)-r)^2}\right)\right]\Bigg|_{r=a} = \frac{1}{b-a}\left.\frac{\partial E_z}{\partial z}\right|_{r=a}$$

and similarly $\frac{\partial}{\partial r}\frac{\partial B_z}{\partial r} = \frac{1}{b-a}\frac{\partial B_z}{\partial r}$

Thus

$$\frac{\delta v_{r\,image}^2}{\delta r} \approx \left(\frac{2}{a} + \frac{1}{b-a}\right) v_{r\,image}^2$$

Figures

Fig. 1 Axial focussing force as a function of Θ ($0 < \Theta \leq 2\pi$ width of ribbon)

Fig. 2 Axial focussing force as a function of N (number of ribbons)

Fig. 3 Axial focussing force as a function of p for single squirrel cage, single cylinder and squirrel cage with internal cylinder ($q = 2p - 1$).

Acknowledgement

The author is grateful to E. Springmann for his carrying out the numerical calculations.

References

1 Z.S. Agronovich et al., The diffraction of electromagnetic waves from plane metallic lattices, Sov. Phys. Vol. 7, No. 4, p. 277 (1962)

2 G.V. Dolbilov et al., Focussing of an electron ring in a collective linear ion accelerator by a system of the squirrel cage type, P9-4737, Dubna (1969)

3 J. Laslett, Incoherent ring image in a circular cylinder, ERAC 38, Symposium on Electron Ring Accelerators, LRL Berkeley (1968)

4 J. Laslett, On the focussing effects arising from the self-fields of a toroidal beam, ERAN 30 (1969), Lawrence Radiation Lab., Berkeley

5 W.A. Perkins, Ion focussing and image focussing during rollout and spillout, ERAN 32 (1969)

6 A.U. Luccio, Electric and magnetic images - tables of fields and gradients, ERAN 35 (1969)

7 J.D. Jackson, Classical Electrodynamics, John Wiley & Sons, New York.

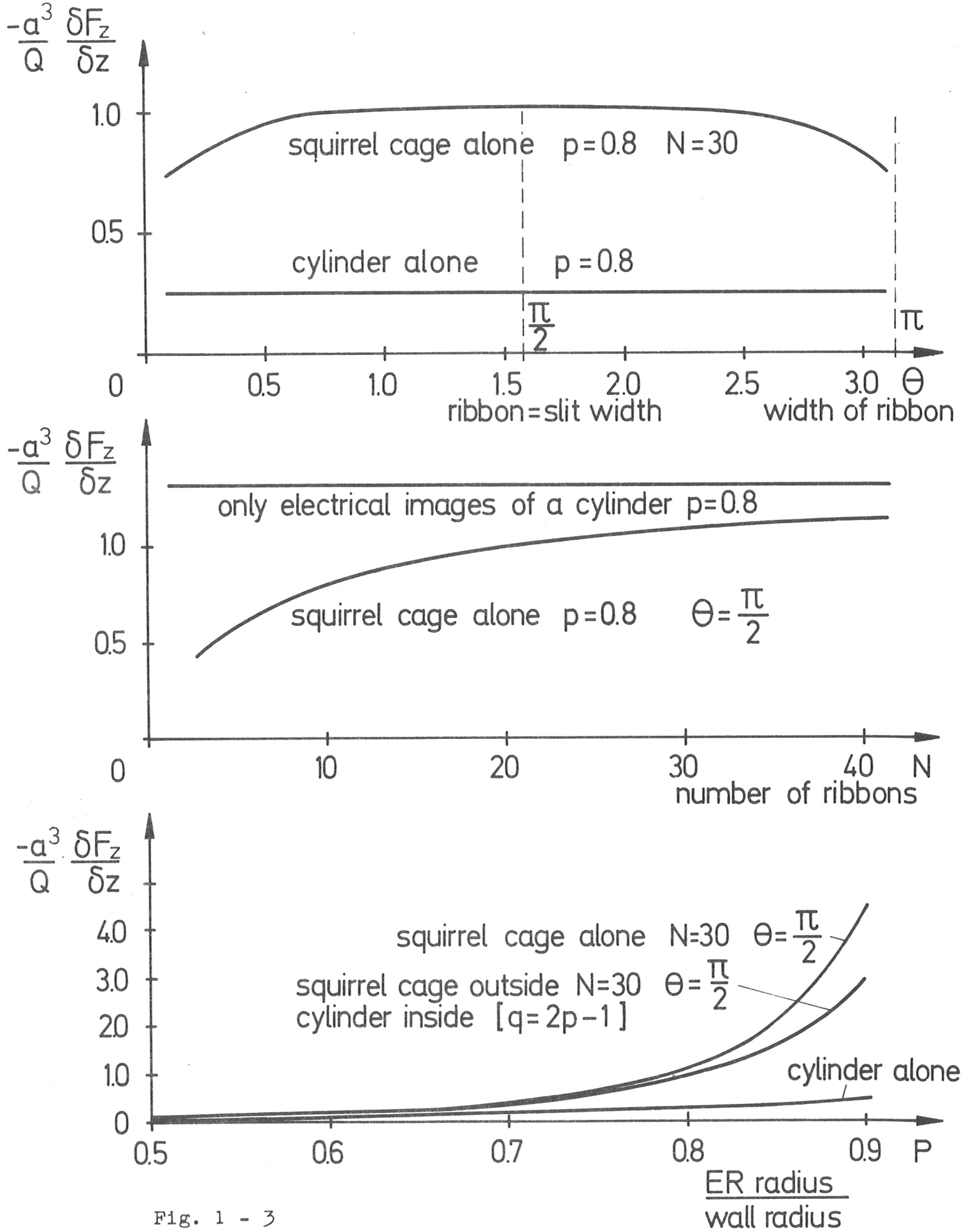
$-\frac{a^3}{Q}\frac{\delta F_z}{\delta z}$
1.0
0.5
squirrel cage alone p=0.8 N=30
cylinder alone p=0.8
$\frac{\pi}{2}$
π
0
0.5
1.0
1.5
2.0
2.5
3.0
Θ
ribbon=slit width
width of ribbon
$-\frac{a^3}{Q}\frac{\delta F_z}{\delta z}$
only electrical images of a cylinder p=0.8
squirrel cage alone p=0.8 $\Theta=\frac{\pi}{2}$
1.0
0.5
0
10
20
30
40
N
number of ribbons
$-\frac{a^3}{Q}\frac{\delta F_z}{\delta z}$
4.0
3.0
2.0
1.0
0
squirrel cage alone N=30 $\Theta=\frac{\pi}{2}$
squirrel cage outside N=30 $\Theta=\frac{\pi}{2}$
cylinder inside [q=2p-1]
cylinder alone
0.5
0.6
0.7
0.8
0.9
P
ER radius
wall radius

Fig. 1 - 3

	$P=\frac{a}{b}$	$\frac{a^3}{Q}\frac{\partial E_z}{\partial z}$	$\frac{a^2}{Q}E_r$	$\frac{a^3}{Q}\frac{\partial E_r}{\partial r}$	$-\frac{a^2}{I}\frac{\partial B_r}{\partial z}$	$-\frac{a}{I}B_z$	$\frac{a^3}{Q}\frac{\partial F_z}{\partial z}$	$\frac{a^2}{Q}F_r$	$\frac{a^3}{Q}\frac{\partial F_r}{\partial r}$	$\epsilon_{1,E}$	$\epsilon_{1,M}$
Squirrel cage alone (b) outside ER $\theta=\frac{\pi}{2}$ N = 30	.6	- .180	.072	.108	.037	.033	- .174	.067	.102	.125	.004
	.65	- .274	.103	.171	.072	.050	- .262	.095	.159	.125	.005
	.70	- .426	.148	.278	.143	.077	- .403	.136	.255	.124	.006
	.75	- .690	.216	.474	.300	.123	- .643	.196	.426	.120	.008
	.80	-1.193	.325	.867	.686	.207	-1.08	.292	.758	.117	.011
	.85	-2.302	.517	1.786	1.822	.384	-2.012	.456	1.496	.113	.014
	.90	-5.469	.911	4.558	6.416	.858	-4.448	.774	3.537	.106	.019
Cylinder alone (b) outside ER	.6	- .190	.072	.114	.598	1.319	- .095	- .134	.019	.132	.066
	.65	- .291	.108	.182	1.059	1.794	- .122	- .177	.014	.132	.077
	.70	- .456	.157	.230	1.890	2.434	- .156	- .231	- .001	.132	.086
	.75	- .748	.230	.518	3.469	3.324	- .196	- .299	- .034	.131	.096
	.80	-1.316	.350	.966	6.727	4.624	- .245	- .386	- .105	.129	.105
	.85	-2.612	.565	2.047	14.48	6.701	- .307	- .502	- .257	.127	.112
	.90	-6.520	1.025	5.495	38.52	10.62	- .390	- .665	- .635	.126	.119

Table 1

	$p=\frac{a}{b}$	$q=\frac{c}{b}$	$\frac{a^3}{Q}\frac{\partial E_z}{\partial z}$	$\frac{a^2}{Q}E_r$	$\frac{a^3}{Q}\frac{\partial E_r}{\partial r}$	$-\frac{a^2}{I}\frac{\partial B_r}{\partial z}$	$-\frac{a}{I}B_z$	$\frac{a^3}{Q}\frac{\partial F_z}{\partial z}$	$\frac{a^2}{Q}F_r$	$\frac{a^3}{Q}\frac{\partial F_r}{\partial r}$	$\epsilon_{1,B}$	$\epsilon_{1,M}$
Squirrel cage outside (b) and cylinder inside (c)	.6	.2	-.308	-.171	.479	.316	-.101	-.258	-.154	.428	.215	.035
	.65	.3	-.471	-.213	.684	.786	-.264	-.346	-.171	.559	.215	.057
	.70	.4	-.732	-.256	.989	1.679	-.530	-.465	-.172	.722	.211	.077
(q=2p-1)	.75	.5	-1.186	-.305	1.491	3.406	-.954	-.644	-.153	.949	.207	.095
N = 30	.80	.6	-2.062	-.365	2.427	7.009	-1.648	-.946	-.103	1.311	.202	.109
$\Theta=\frac{\pi}{2}$	.85	.7	-4.035	-.451	4.485	15.70	-2.877	-1.537	.007	1.988	.197	.122
	.90	.8	-9.864	-.610	10.47	43.27	-5.419	-2.977	.253	3.587	.191	.133
Cylinder (b) outside and cylinder (c) inside	.6	.2	-.316	-.165	.481	.836	1.12	-.183	-.344	.348	.221	.092
	.65	.3	-.485	-.205	.689	1.644	1.338	-.223	-.417	.428	.221	.119
	.70	.4	-.756	-.243	.999	3.103	1.560	-.263	-.492	.506	.218	.142
(q = 2p - 1)	.75	.5	-1.232	-.284	1.517	5.830	1.803	-.305	-.571	.589	.215	.162
	.80	.6	-2.160	-.329	2.490	11.36	2.080	-.352	-.660	.681	.212	.177
	.85	.7	-4.282	-.384	4.666	24.34	2.416	-.408	-.768	.792	.209	.189
	.90	.8	-10.69	-.456	11.15	64.17	2.865	-.482	-.911	.938	.207	.198

Table 2

	$P=\frac{a}{b}$	$q=\frac{c}{b}$	$\frac{a^3}{Q}\frac{\partial E_z}{\partial z}$	$\frac{a^2}{Q}E_r$	$\frac{a^3}{Q}\frac{\partial E_r}{\partial r}$	$-\frac{a^2}{I}\frac{\partial B_r}{\partial z}$	$-\frac{a}{I}B_z$	$\frac{a^3}{Q}\frac{\partial F_z}{\partial z}$	$\frac{a^2}{Q}F_r$	$\frac{a^3}{Q}\frac{\partial F_r}{\partial r}$	$\epsilon_{1,E}$	$\epsilon_{1,M}$
Squirrel cage outside (b) and cylinder inside (c) N=30 $\Theta=\pi/2$	0.8	.1	-1.216	.248	.968	.713	.192	-1.102	.217	.855	.119	.011
	"	.2	-1.234	.206	1.029	.818	.138	-1.104	.184	.898	.121	.013
	"	.3	-1.266	.150	1.116	1.062	.025	-1.097	.146	.947	.124	.016
	"	.4	-1.333	.066	1.267	1.604	-.193	-1.077	.097	1.011	.131	.025
	"	.5	-1.500	-.076	1.576	2.924	-.632	-1.035	.024	1.111	.147	.046
	"	.6	-2.062	-.365	2.427	7.009	-1.648	-.946	-.103	1.311	.202	.109
	"	.7	-5.603	-1.197	6.799	30.33	-5.104	-.775	-.385	1.972	.550	.474
Cylinder outside (b) and cylinder inside (c)	"	.1	-1.338	.275	1.062	6.739	4.602	-.265	-.457	-.0102	.131	.105
	"	.2	-1.355	.234	1.121	6.788	4.523	-.275	-.486	.041	.133	.106
	"	.3	-1.385	.180	1.205	6.911	4.361	-.285	-.514	.106	.136	.108
	"	.4	-1.450	.098	1.351	7.227	4.052	-.299	-.547	.201	.142	.113
	"	.5	-1.610	-.043	1.654	8.119	3.443	-.319	-.591	.361	.158	.127
	"	.6	-2.160	-.329	2.490	11.36	2.080	-.352	-.660	.681	.212	.177
	"	.7	-5.668	-1.163	6.831	32.94	-2.218	-.426	-.810	1.588	.556	.515

Table 3